Cold atomic media with ultrahigh optical depths

Ya-Fen Hsiao,[1,2] Hung-Shiue Chen,[1] Pin-Ju Tsai,[1,3] and Ying-Cheng Chen[1,4,*]
[1]*Institute of Atomic and Molecular Sciences, Academia Sinica, Taipei 10617, Taiwan*
[2]*Molecular Science Technology, Taiwan International Graduate Program, Academia Sinica and National Central University, Taiwan*
[3]*Department of Physics, National Taiwan University, Taipei 10617, Taiwan*
[4]*Department of Physics, National Tsing Hua University, Hsinchu 30043, Taiwan*
(Received 1 September 2014; published 5 November 2014; corrected 17 November 2014)

We present an experimental study to achieve ultrahigh optical depths for cold atomic media with a two-dimensional magneto-optical trap (MOT) of cesium. By combining large atom number, a temporally dark and compressed MOT, and Zeeman-state optical pumping, we achieve an optical depth of up to 1306 for the open transition of the cesium D_1 line. Our work demonstrates that it is feasible to push the optical depth up to the 1000 level with a convenient MOT setup. This development paves the way to many important proposals in quantum optics and many-body physics.

DOI: 10.1103/PhysRevA.90.055401 PACS number(s): 37.10.De, 42.50.Gy, 37.10.Gh

Optical depth (OD, denoted as D), defined by $D = n\sigma L$, is a crucial parameter for many experiments, where n is the atomic density, σ is the absorption cross section and L is the sample length. For example, the optical buffer application based on the slow-light effect associated with electromagnetically induced transparency (EIT) requires a large OD to increase the crucial parameter: the delay bandwidth product [1]. In quantum memory applications, the ultimate parameter that determines the memory efficiency is OD [2]. In EIT-based photon-pair generation, the pair-generation rate and paired probability is monotonically proportional to the OD [3]. In low-light-level nonlinear optics, a high OD helps to increase the efficiency of the nonlinear interactions [4–6]. In proposals of many-body physics with dark-state polariton [7,8] and superradiance [9–11], a high OD is also a requirement.

The magneto-optical trap (MOT) [12] has become a workhorse to provide cold atoms for the studies of quantum optics and many-body physics. How to increase the OD of atom clouds in a MOT is an important task. There have been some reports of ODs larger than 100 based on two-dimensional MOTs [4,5,13,14]. Recently, Sparkes *et al.* reported achieving an OD of ∼1000 at the cycling transition of rubidium atoms [15]. Blatt *et al.* reported achieving an optical depth of ∼1000 for the open transitions of rubidium loaded into a hollow-core photonic-crystal fiber from a MOT [16]. Here, we report achieving an OD of up to 1306 for the $|F = 3\rangle \rightarrow |F' = 4\rangle$, σ^+ transition of the cesium D_1 line. To the best of our knowledge, this is the largest OD to date for cold atomic media. Our work demonstrates that it is feasible to push the OD up to the 1000 level with a convenient MOT setup. This development opens up the opportunity to realize many important proposals in quantum optics and many-body physics.

From the definition of OD, it is evident that OD can be increased by choosing a transition with a favorable absorption cross section, increasing the atomic density and increasing the sample length. For alkali-metal atoms, the cycling transition of the D_2 line has the largest absorption cross section. However, it is impossible to implement EIT, which some proposals are based on, with a cycling transition. For open transitions of cesium, the $|F = 3, m = 3\ (-3)\rangle \rightarrow |F' = 4, m = 4\ (-4)\rangle$, σ^+ (σ^-) transition and the $|F = 4, m = 4\ (-4)\rangle \rightarrow |F' = 3, m = 3\,(-3)\rangle, \sigma^-$ (σ^+) transition of the D_1 line have the same and largest absorption cross section [17]. To take advantage of this, it is required to perform both the hyperfine- and Zeeman-state optical pumping to prepare population in the desired state. To increase the sample length, many teams have implemented the two-dimensional MOT to produce cigar-shaped atom clouds with a sample length of 1 to 2 cm [4,13,14,18–20]. A typical technique to increase the atomic density is to use either the temporally or spatially dark MOT in addition to magnetic compression [21–23]. To maximize the atomic density, it is also important to start with a large number of atoms, greater than that ultimately used to perform the compression [24]. We have carefully implemented all these techniques to obtain ultrahigh ODs.

Our experiment is based on a glass vapor-cell MOT of cesium with a pair of rectangular-shaped quadruple magnetic coils [13]. The coils generate a line of zero magnetic field where cigar-shaped atom clouds are trapped. Figures 1(a) and 1(b) depict the laser excitations involved and show a schematic diagram of the experimental setup, respectively. We refer to the long axis of the atom clouds as the z axis. The gradient of the magnetic field along the x and y axes are both ∼9 G/cm. The trapping beam, red detuned by 12 MHz, has a total power of up to 330 mW after a single-mode fiber. The beam is expanded to a diameter of 22 mm and then split into eight independent beams to form the MOT via many sets of half wave plates and polarizing beam splitter (PBSs). Two pairs of trapping beams counterpropagate in the horizontal plane and intersect with the z axis by 45°. A pair of trapping beams counterpropagate in the vertical direction (x axis). We add two additional trapping beams counterpropagating in the y axis to enhance the optical confinement force in this direction. We emphasize that none of the trapping beams intersects with the z axis by a small angle such that the attenuation of any trapping beam due to the atomic absorption is not significant. This arrangement allows a longer cloud length due to the reduced effect of absorption-induced trapping [19]. The repumping beam, which drives the $|F = 3\rangle \rightarrow |F' = 4\rangle$ transition of the D_2 line, has a power of 50 mW and a diameter of

*chenyc@pub.iams.sinica.edu.tw

 ©2014 American Physical Society

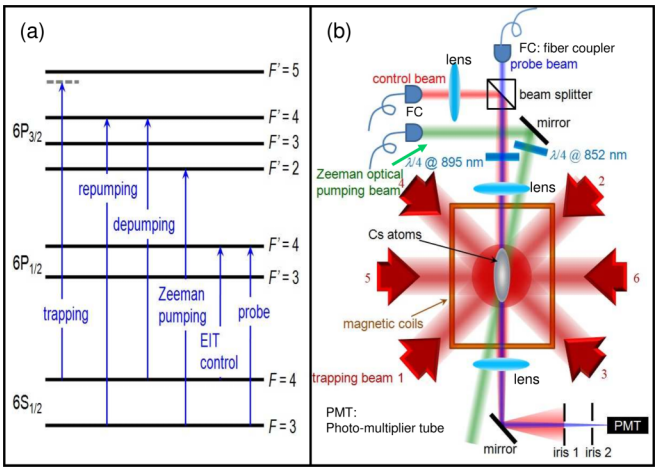

FIG. 1. (Color online) (a) Relevant energy levels for ^{133}Cs atoms and laser excitations. (b) Schematic experimental setup. Trapping beams 7 and 8 are in and out of the plane of the page. The repumping (depumping) beam is overlapped with trapping beams 1 and 2 (5 and 6) because it is coupled into the MOT through the PBS that splits these two beams.

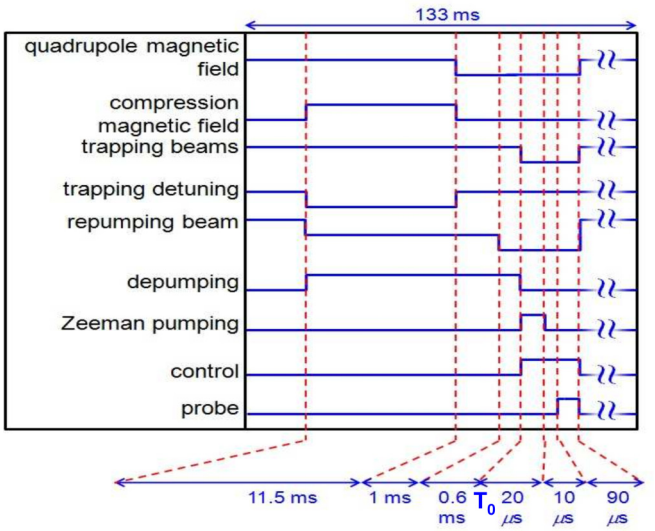

FIG. 2. (Color online) Timing diagram of experiment.

$\sim$20 mm. We can trap up to 1×10^{10} atoms with a MOT loading time of $\sim$1 to 2 s. The maximum size of the atom cloud is $\sim 3 \times 3 \times 14$ mm^3. The OD for the $|F = 3\rangle \rightarrow |F' = 4\rangle$, σ^+ transition of the D_1 line for a plain MOT is around 50 to 60.

To improve the performance of the temporally dark MOT, we prepare a depumping beam which drives the $|F = 4\rangle \rightarrow |F' = 4\rangle$ transition of the D_2 line. The power of the depumping beam is up to 12 mW with a diameter of $\sim$15 mm. One laser beam, which drives the $|F = 3\rangle \rightarrow |F' = 2\rangle$ transition of the D_2 line, is used to perform the Zeeman-state optical pumping. The power of the Zeeman-pumping beam is up to 20 mW and its diameter is 5 mm. It is nearly circularly polarized. It intersects the z axis by about $\sim 4^\circ$ to induce both σ^+ and π transitions, with the Zeeman state $|F = 3, m = 3\rangle$ being the only dark state [25]. Because the setup is designed for EIT-related experiments [4,6,26], we have prepared EIT control and probe beams which drive the $|F = 4\rangle \rightarrow |F' = 4\rangle$ and $|F = 3\rangle \rightarrow |F' = 4\rangle$ transition of the D_1 line, respectively. The control and probe beams both propagate along the z axis with an angle of $\sim 1^\circ$ between them. The probe beam is focused to a waist of 60 μm at the center of the atom cloud. To allow the EIT spectral measurement, the probe beam passes through one acousto-optic modulator (AOM) in a double-pass configuration. By varying the rf driving frequency of the AOM, the frequency scan range of the probe field is up to 100 MHz. The control beam is collimated around the atom cloud with a diameter of $\sim$1 mm. The power of the control beam is up to 2 mW. The power of the probe beam is $\sim$10 nW and is detected by a photomultiplier tube (Hamamatsu R 630-10). Some irises are used to filter out the control beam with an extinction ratio of better than 56 dB.

The timing diagram is shown in Fig. 2. The trapping beam is turned off at the time denoted by T_0 for 120 μs with a repetition rate of 7.5 Hz. We turn off the quadruple magnetic field via two electronic switches connected to both ends of one power supply. Although the current can be turned off quickly with an exponential decay time of $\sim$200 μs, the induced eddy current of the surrounding metallic components may have a longer decay time. To reduce its perturbation in EIT experiments, the quadruple magnetic field is turned off at $T_0 - 1.6$ ms. To implement the magnetic compression, another power supply is also connected to the quadrupole magnetic coils with two electronic switches. It is turned on at $T_0 - 12.1$ ms with a duration of 11.5 ms. This 11.5 ms duration is the temporally dark and compressed MOT stage. At time $T_0 - 12.1$ ms, the repumping intensity is reduced to a smaller value and the depumping beam is also turned on for the cases where it is needed to be on. The repumping beam is turned off at $T_0 - 0.6$ ms. The depumping beam is turned off at T_0. During the 0.6 ms period before T_0, the repumping beam is off and the trapping and depumping beams are on to pump the population into the $|F = 3\rangle$ ground state. At time T_0, the Zeeman pumping beam is on for 20 μs and the EIT control beam is on for 120 μs. At time $T_0 + 30$ μs, the EIT probe beam is on for 90 μs. The power of the probe beam between $T_0 + 35$ μs and $T_0 + 40$ μs is recorded. The probe powers with the MOT on and off are divided to determine the probe transmission. By repeating the timing sequence and gradually varying the probe frequency, the EIT spectrum can be obtained.

To determine the OD, we fit the spectrum to an EIT lineshape given by

$$T = \exp\left[D\frac{\Gamma}{2}\mathrm{Im}\left(\frac{i[i(\delta_p - \delta_c) - \gamma]}{[i(\delta_p - \delta_c) - \gamma]\left[i\delta_p - \left(\frac{\Gamma}{2} + \gamma\right)\right] + \frac{\Omega_c^2}{4}}\right)\right], \quad (1)$$

where D is the on-resonance OD, $\delta_{p(c)}$ is the probe (control) detuning from its resonance, $\Gamma = 2\pi \times 4.575$ MHz is the spontaneous decay rate of the cesium D_1 line [17], γ is the decay rate of the ground-state coherence, Ω_c is the Rabi frequency of the control field, and Im() stands for the imaginary part of the relation inside the bracket. The fitting parameter D is mainly constrained by the detuning range where the probe transmission curve starts to turn from essentially zero to nonzero near the edges of the spectrum. It is important

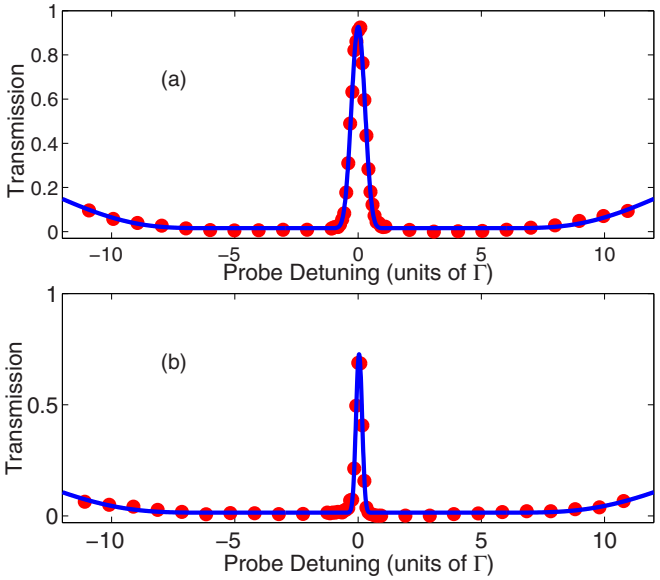

FIG. 3. (Color online) (a) A representative EIT spectrum. This spectrum corresponds to the rightmost data point in Fig. 4(d). The blue line is a fit to the EIT lineshape. The fit parameters $\{D, \Omega_c, \gamma\}$, are $\{1056\,(88), [5.06\,(0.10)]\Gamma$, and $[0.0009\,(0.0002)]\Gamma\}$, respectively. Quantities shown in the bracket are the 2σ uncertainty of the fitting parameters. (b) The EIT spectrum for the largest OD achieved. The fit parameters $\{D,\Omega_c,\gamma\}$ are $\{1306\ (117),\ [3.57\ (0.09)]\Gamma$, $[0.0016\ (0.0002)]\Gamma\}$, respectively.

that the scan range of the probe frequency be large enough to cover this turnover. In most of the cases in our experiment, the probe scan range of ∼100 MHz is quite enough. With an OD up to 1306 as shown in Fig. 3(b), this scan range is just barely enough. An AOM with a larger bandwidth is required for the cases with even higher ODs. The probe intensity needs to be much lower than the saturation intensity of the probe transition such that the absorption is in a linear regime where Eq. (1) is valid. The uncertainties of the fitting parameters depend on the fluctuation of the data in the EIT spectrum. To minimize the fluctuation, we performed 32 times averaging on the transmission measurement. Typical 2σ standard deviation for the fitting parameter D is less than 10% of its fit value with the two representative examples shown in Fig. 3.

Generally speaking, all techniques used to increase the OD need to be carefully implemented and optimized in order to obtain an ultrahigh OD. Before discussing our systematic study of the OD optimization, we emphasize some crucial points: First, we use a relatively high trapping power in our MOT. With a higher trapping power, the number of trapped atoms is larger, which results in a longer atom cloud in the z axis. The large initial atom number is also important to obtain a high atomic density in the transient compression of an MOT. The reason for this is well explained in Ref. [24]. Starting with an atom number more than ultimately needed, replenishment of atoms into the central compressed volume causes an increase in density for some time until the collision losses dominate and the density finally decreases. Second, we found that careful adjustments of the total trapping power into different pairs of trapping beams and fine tuning of the beam balance between each pair are crucial. With a proper balance, the atom cloud is pushed inward with its center-of-mass position fixed. Otherwise, the center-of-mass position of the cloud moves with a little increase in density. Third, it is desirable to turn off the inhomogeneous quadruple magnetic field of the MOT to reduce the ground-state decoherence rate γ. However, this also results in a ballistic expansion of the trapped atoms and thus a reduction in the atomic density. There is a tradeoff between obtaining a low γ and a large OD. To enjoy both a large OD and a low γ, the key is to turn off the quadruple magnetic field quickly and to minimize the induced eddy current. Careful design of the switching electronics and minimizing the use of metallic components near the MOT region are crucial. Empirically, we found that an increase of 0.5 ms free flight time causes a reduction in OD of ∼35% in our system.

Starting from a plain MOT, we then perform the techniques which lead to sequential improvement of the OD. Figure 4(a) depicts OD versus the repumping intensity during the temporal dark MOT period. Reducing the repumping intensity causes the shelving of some portions of the population into the dark $|F = 3\rangle$ hyperfine ground state. This occurs as a consequence of the off-resonance excitations of the trapping beams to the $6P_{3/2}, |F' = 4\rangle$ excited state and the following spontaneous decay into the $|F = 3\rangle$ ground state. The atomic density increases due to the reduction of the density-limiting mechanisms such as radiation trapping and light-assisted cold-collision losses [23]. However, if the repumping beam is too weak, the atomic density starts to decrease again because of a significant reduction in the trapping force. Therefore, there is an optimum repumping intensity that maximizes the OD [23]. The maximum OD improvement obtained is about a factor of two, as shown in Fig. 4(a).

Due to the relatively large splitting in the excited-state hyperfine levels for cesium, the off-resonant pumping of the population to the $|F = 3\rangle$ ground state by the trapping beams is not very efficient. It is essential to add a depumping beam to help the hyperfine-state pumping process [23]. With the

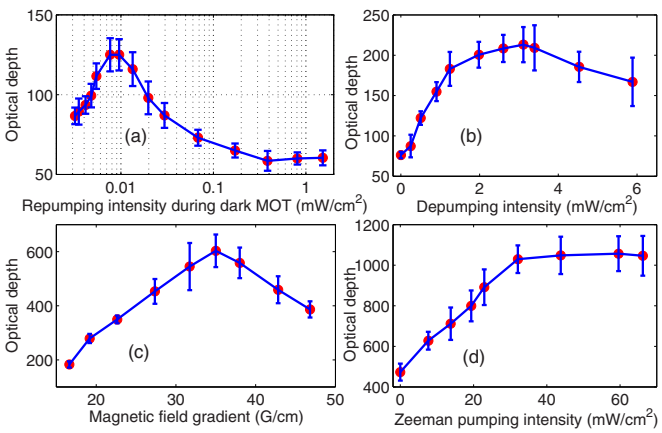

FIG. 4. (Color online) (a) OD vs repumping intensity during the dark-MOT period. (b) OD vs depumping intensity. (c) OD vs the radial gradient of the quadruple magnetic field of the MOT during the compression period. (d) OD vs the intensity of the Zeeman optical pumping beam.

depumping on, we found that the optimum repumping intensity during the dark-MOT period shifts to a higher value. In fact, this is an optimization problem with two parameters. Although we did not exhaustively explore the complete parameter space, we found that the maximum ODs do not vary too much ($<15\%$) for various sets of optimized repumping and depumping intensities. Figure 4(b) depicts an example of OD vs the depumping power with a repumping intensity of $0.03\,\mathrm{mW/cm^2}$ during the dark-MOT period. The maximum OD is further improved by a factor of $\sim$1.7, compared to the best OD without a depumping beam.

With the optimized repumping and depumping parameters, we then perform the magnetic compression. We also optimize the trapping detuning during this period. The optimized detuning is typically around -16 MHz. Figure 4(c) depicts OD vs the magnetic gradient of the quadruple field of the MOT during the compressed MOT period. Compared to the case without compression, there is an improvement in the maximum OD by about a factor of three. We then apply the Zeeman-state optical pumping. The pulse duration of the Zeeman-pumping beam is fixed to 20 μs. It was found that we have to compensate the stray magnetic field to a few mG in order to obtain a good result. A light storage technique based on adiabatically turning the EIT control field off and on is used to diagnose the stray magnetic field [27]. A longer storage time corresponds to a better compensation. Figure 4(d) depicts OD versus the intensity of the Zeeman pumping beam. The OD approaches a maximum value when the intensity of the pumping beam increases. At the saturation power, fine tuning on the polarization or alignment of the Zeeman pumping beam can further increase the OD. According to the Clebsch–Gordan coefficients of cesium [17] and assuming that the initial population is randomly distributed among the Zeeman manifold of the $|F = 3\rangle$ ground state, the OD can be increased by a factor of 2.3 if all populations are optically pumped to the rightmost (leftmost) Zeeman state. In the case of Fig. 4(d), the OD is improved by a factor of 2.2.

With the four procedures mentioned above, there is a more than twenty-fold improvement in OD. Starting with an OD of $\sim$50 to 60 in a plain MOT, it is clear that the final OD can be larger than 1000, as is shown in Fig. 4(d). Under the best conditions, the largest OD obtained was 1306 (117), as shown in Fig. 3(b). In summary, we demonstrated a feasible strategy to obtain an OD of larger than 1000 for an open transition of cesium by a convenient MOT setup. This development may have strong impacts on future studies in quantum optics and many-body physics.

This work was supported by Ministry of Science and Technology of Taiwan under Grants No. 101-2112-M-001-014-MY2 and No. 103-2112-M-001-010-MY3.

[1] R. S. Tucker, P.-C. Ku, and C. J. Chang-Hasnain, J. Lightwave Technol. **23**, 4046 (2005).
[2] A. V. Gorshkov, A. André, M. Fleischhauer, A. S. Sørensen, and M. D. Lukin, Phys. Rev. Lett. **98**, 123601 (2007).
[3] P. Kolchin, Phys. Rev. A **75**, 033814 (2007).
[4] B.-W. Shiau, M.-C. Wu, C.-C. Lin, and Y.-C. Chen, Phys. Rev. Lett. **106**, 193006 (2011).
[5] Y.-H. Chen, M.-J. Lee, W. Hung, Y.-C. Chen, Y.-F. Chen, and I. A. Yu, Phys. Rev. Lett. **108**, 173603 (2012).
[6] C.-C. Lin, M.-C. Wu, B.-W. Shiau, Y.-H. Chen, I. A. Yu, Y.-F. Chen, and Y.-C. Chen, Phys. Rev. A **86**, 063836 (2012).
[7] M. Fleischhauer, J. Otterbach, and R. G. Unanyan, Phys. Rev. Lett. **101**, 163601 (2008).
[8] J. Otterbach, and R. G. Unanyan, and M. Fleischhauer, Phys. Rev. Lett. **102**, 063602 (2009).
[9] T. Wang, S. F. Yelin, R. Coté, E. E. Eyler, S. M. Farooqi, P. L. Gould, M. Koštrun, D. Tong, and D. Vrinceanu, Phys. Rev. A **75**, 033802 (2007).
[10] A. A. Svidzinsky, J.-T. Chang, and M. O. Scully, Phys. Rev. Lett. **100**, 160504 (2008).
[11] G.-D. Lin and S. F. Yelin, Phys. Rev. A **85**, 033831 (2012).
[12] E. L. Raab, M. Prentiss, A. Cable, S. Chu, and D. E. Pritchard, Phys. Rev. Lett. **59**, 2631 (1987).
[13] Y.-W. Lin, H.-C. Chou, P. P. Dwivedi, Y.-C. Chen, and I. A. Yu, Opt. Express **16**, 3753 (2008).
[14] S. Zhang, J. F. Chen, C. Liu, S. Zhou, M. M. T. Loy, G. K. L. Wong, and S. Du, Rev. Sci. Instrum. **83**, 073102 (2012).
[15] B. M. Sparkers, J. Bernu, M. Hosseini, J. Geng, Q. Glorieux, P. A. Altin, P. K. Lam, N. P. Robins, and B. C. Buchler, New J. Phys. **15**, 085027 (2013).
[16] F. Blatt, T. Halfmann, and T. Peters, Opt. Lett. **39**, 446 (2014).
[17] http://steck.us/alkalidata, D. A. Steck, Cesium D line data.
[18] M. Vengalattore, W. Rooijakkers, and M. Prentiss, Phys. Rev. A **66**, 053403 (2002).
[19] J. A. Greenberg, M. Oria, A. M. C. Dawes, and D. J. Gauthier, Opt. Express **15**, 17699 (2007).
[20] S. Du, P. Kolchin, C. Belthangady, G. Y. Yin, and S. E. Harris, Phys. Rev. Lett. **100**, 183603 (2008).
[21] W. Ketterle, K. B. Davis, M. A. Joffe, A. Martin, and D. E. Pritchard, Phys. Rev. Lett. **70**, 2253 (1993).
[22] W. Petrich, M. H. Anderson, J. R. Ensher, and E. A. Cornell, J. Opt. Soc. Am. B **11**, 1332 (1994).
[23] C. G. Townsend, N. H. Edwards, K. P. Zetie, C. J. Cooper, J. Rink, and C. J. Foot, Phys. Rev. A **53**, 1702 (1996).
[24] M. T. DePue, S. L. Winoto, D. J. Han, and D. S. Weiss, Opt. Commun. **180**, 73 (2000).
[25] V. Vuletić, C. Chin, A. J. Kerman, and S. Chu, Phys. Rev. Lett. **81**, 5768 (1998).
[26] Y.-F. Hsiao, P.-J. Tsai, C.-C. Lin, Y.-F. Chen, I. A. Yu, and Y.-C. Chen, Opt. Lett. **39**, 3394 (2014).
[27] T. Peters, Y.-H. Chen, J.-S. Wang, Y.-W. Lin, and I. A. Yu, Opt. Express **17**, 6665 (2009).